Asian Journal of Chemistry; Vol. 36, No. 1 (2024), 215-222

ASIAN JOURNAL OF CHEMISTRY

https://doi.org/10.14233/ajchem.2024.30750

Interaction Mechanism of Hesperidin and L-Tryptophan: A Experimental and Molecular Docking Studies

A. KANIMOZHI and S. BAKKIALAKSHMI*

Department of Physics, Annamalai University, Annamalai Nagar-608002, India

*Corresponding author: E-mail: bakkialakshmis@rocketmail.com

Received: 25 October 2023; *Accepted*: 6 December 2023; *Published online*: 31 December 2023; AJC-21506

The binding of L-tryptophan (L-Trp) and hesperidin (HES) was investigated by UV, fluorescence, synchronous fluorescence, time-resolved fluorescence, Fourier transform infrared (FTIR) spectroscopies, FRET, antibacterial activity, anticancer activity and molecular docking study. The flavonoid glycoside known as hesperidin has been shown to have therapeutic properties for a variety of disorders, including cancer diseases. Its low solubility and bioavailability cause it to be little absorbed, which means that a delivery mechanism is necessary in order for it to reach its therapeutic goal. Fluorescence data revealed that the fluorescence quenching mechanisms of L-Trp by hesperidin are all static quenching procedures. Synchronous fluorescence spectroscopy shows the interaction between hesperidin and L-Trp changes the hydrophobicity of the microenvironment of tryptophan (Trp) residues. The anticancer activity effect of hesperidin and L-Trp on human cervical cancer cell lines was assessed using MTT and crystal violet assays.

Keywords: L-Tryptophan, Hesperidin, Fluorescence, Antibacterial activity, Anticancer activity, Molecular docking.

INTRODUCTION

In addition to its role in plant and animal development, an essential amino acid tryptophan (Trp) is involved in the synthesis of proteins and peptides [1]. The identification of amino acids is essential for clinical and pharmacological research, as well as for evaluating the nutritional value of food products [2,3]. Tryptophan (Trp) has been utilized as a fluorescence probe because of its strong fluorescence [4,5]. Moreover, due to the functional and structural significance of interactions in chemistry and biology, the indole rings of Trp have lately been a topic of substantial studies [6]. It is reported that few neurobehavioural impacts, HIV infections, malignancies, Alzheimer's and Parkinson's disease are all significantly affected by the tryptophan content [7-9]. Fluorescence quenching is the process of reducing a fluorophore's quantum amount of fluorescence through a variety of chemical interactions with the quencher molecules [10,11]. The fluorescence of proteins, commonly utilized for the diagnostic purposes to analyze their structure, is known to be induced by the activation of specific amino acid residues, particularly the L-residues [12]. Because of its high absorption extinction coefficient and efficient fluorescence, tryptophan predominates in the fluorescence spectra of the majority of proteins that contain tryptophan [13].

Several articles [14-19] reported the binding of L-tryptophan with plasma proteins, a crucial step in its general digestion *in vivo*. Due to their importance as building blocks in living systems, the proximity of free amino acids concentrations to various physiological processes and the metabolic pathways of proteins and peptides, there has been an an increase in interest in their detection across several disciplines, such as clinical chemistry, biochemistry and pharmaceutical chemistry [20-23]. This is because the 20 natural amino acids serve a vital role in daily living [24-26].

A bioflavonoid glycoside called hesperidin is abundantly present in various citrus fruits [27]. It has pharmacological features including anti-inflammatory, antiviral and anticancer properties [28,29]. Hesperidin, for instance, has reduced the risk of reactive oxygen species levels in Parkinson's disease in mice [30]. Hesperidin is currently reported to be effective in treating various central system illnesses and has antidepressant-like effects in animal models [31]. Long-term epidemiological studies have shown that persons who consistently consume diets high in flavonoids have a lower risk of developing cancer

and other chronic diseases [32], which has increased interest in using these substances as food supplements to treat cancer patients [33]. High level of hesperidin derived from citrus fruits have been demonstrated to have protective effects against oxidative stress, inflammation and hypoglycaemia [34]. Recent studies also revealed that hesperidin has an efficient antioxidative, anti-obesity and anticancer function [35,36].

Keeping in mind about the biological importance of L-Trp and hesperidin, an interaction studies of between these molecules has been studied. The structural changes of L-Trp were assisted by UV/visible spectroscopy, steady-state fluorescence analysis, synchronous fluorescence analysis, and time-resolved analysis. Furthermore, FTIR analysis was used to examine the impact of polyphenols on the secondary structure of proteins. In addition, the antibacterial and anticancer activities of the polyphenols, as well as their ability to bind to molecules for HES were performed using docking studies.

EXPERIMENTAL

L-Tryptophan reagent grade (≥ 98%) and hesperidin (≥ 80%) were purchased from Sigma-Aldrich Chemical Co. A stock solutions of L-Trp (10^{-4} M) and hesperidin (10^{-5} M) were prepared with distilled water. These solutions were prepared swiftly before the absorption and fluorescence measurements had been performed.

Characterization: A Shimadzu 1800 PC UV/VIS spectrophotometer was utilized to record the absorption spectra in the range of 200-400 nm. Fluorescence spectra of each solution were recorded between 280 and 800 nm using an RF-5301 PC (Shimadzu Corporation, Kyoto, Japan) fluorescence spectrophotometer. Fluorescence decay measurements were recorded using Spectrofluometer make Jobin Yvon model fluoro-log–FL3-11 spectrofluometer. The FTIR (Perkin-Elmer model) spectra were recorded in a liquid sample of L-tryptophan with hesperidin in the wavelength range of 4000-400 cm^{-1} .

RESULTS AND DISCUSSION

UV-visible spectroscopic studies: The absorbance of the L-Trp solution is clearly visible at a wavelength of 280 nm when the UV-Vis spectra was obtained with hesperidin in L-Trp (Fig. 1). The concentration of hesperidin in distilled water increased from 0.0 to 1.0 mol L^{-1} as the intensity of L-Trp increased. The UV-visible absorption spectra demonstrated that the quenching procedure employed for L-tryptophan and hesperidin was static. In other words, L-Trp and hesperidin interacts to form a stable complex, which correlate with the findings of the fluorescence experiment.

Fluorescence quenching mechanism: The quenching of L-Trp fluorescence by adjusting the concentration of quencher hesperidin in an aqueous solution to mimic biological circumstances has been investigated. L-Trp availability to the quencher can be determined through the quantification of its intrinsic

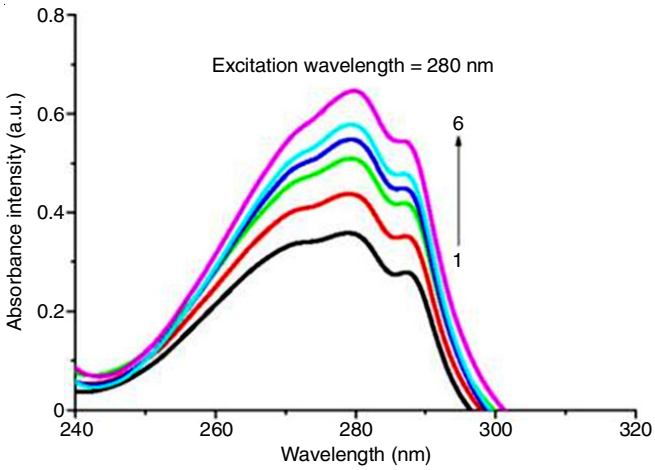

Fig. 1. UV/vis absorption spectra of L-tryptophan with different concentrations of hesperidin (mol L^{-1}) (1) 0.0, (2) 0.2, (3) 0.4, (4) 0.6, (5) 0.8 and (6) 1.0

fluorescence. This comprehension facilitates the anticipation of the HES-L-Trp binding process. Tyrosine steady-state fluorescence was observed following the addition of aliquots. As predicted, as the concentration of hesperidin increased, the fluorescence intensity of the L-Trp solution steadily reduced.

With a maximum emission wavelength of 354 nm, L-Trp exhibits intense fluorescence. Hesperidin interaction does not alter the environment of amino acid fluorophores, as shown by the absence of a spectral shift in the L-Trp fluorescence emission spectra following the hesperidin quenching. This suggested that the interaction between L-trp and hesperidin resulted in alterations to the fluorophores and quenching of fluorescence. The collision between the fluorophore and a quencher causes dynamic quenching, whereas the formation of a non-fluorescent compound in the fluorophore's ground state causes static quenching. The intrinsic fluorescence of L-Trp was quenched by hesperidin in a concentration-dependent manner without altering the emission maximum or peak shape. The Stern-Volmer equation was used to examine the fluorescence quenching data as shown below:

$$\frac{F_O}{F} = 1 + K_q \tau_0 [Q] = 1 + K_{SV}[Q] \quad (1)$$

where F_O and F are the fluorescent molecules without and with quenchers, respectively; K_q is the quenching rate constant; τ_0 is the initial average life of fluorescent molecules; K_{SV} is the Stern-Volmer quenching constant, which is equal to $K_q \tau_0$ and [Q] is the concentration of quenchers. The values of L-Trp, hesperidin quenching (K_q) and the Stern-Volmer (K_{SV}) constants are shown in Table-1.

The Stern-Volmer plot (Fig. 2b) would exhibit an ascending curve if the quenching was caused by the formation of complex and dynamic collisions. However, the linear correlation between F_O/F and [Q] suggests that the quenching process is either static, unidirectional or dynamic. The quenching types

TABLE-1
STERN-VOLMER (KSV) AND BIO-MOLECULAR QUENCHING RATE CONSTANT (K_q) OF L-TRP WITH HESPERIDIN

Quencher	$K_{SV} \times 10^{-5}$ (L mol^{-1})	K_q (L $mol^{-1}s^{-1}$)	Correlation coefficient (R)	Standard deviation (S.D.)
Hesperidin	0.80	2.15×10^{13}	0.99	0.51

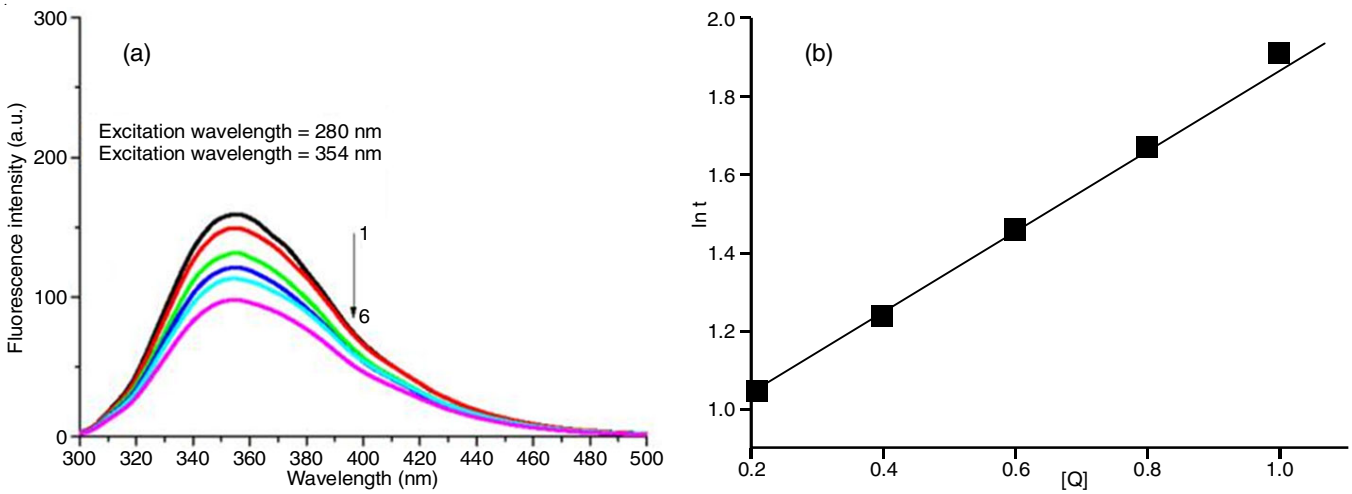

Fig. 2. (a) Steady-state fluorescence spectra of L-Trp with different concentrations of hesperidin (mol L^{-1}) (1) 0.0, (2) 0.2, (3) 0.4, (4) 0.6, (5) 0.8, (6)1.0; (b) Stern-Volmer plot of L-Trp with hesperidin

of L-Trp and hesperidin both belonged to static quenching because their K_q values were all much higher than the maximal quenching constant brought on by collision (2.15×10^{13} L mol^{-1} s^{-1}). On the other hand, L-Trp had a greater K_q value than hesperidin, indicating a potent quenching effect.

Synchronous fluorescence spectroscopy: The molecular surroundings of the molecules in the chromosphere are revealed by the synchronous fluorescence spectra. The spectral features of tyrosine residues were observed at 15 nm and tryptophan residues at 60 nm, respectively [37]. By simultaneously adjusting the emission and excitation wavelengths, the spectra are greatly enhanced and the fluorescence is limited to the components excited at wavelengths which are synchronously following the emission. The experimentally recorded emission spectra exhibit significantly narrower peak half-widths when synchronously stimulated [38]. The effect of hesperidin on L-Trp and hesperidin is shown in Fig. 3.

In this study, the bonding sites of L-Trp and hesperidin molecules were identified using the different ratios of synchronous fluorescence quenching. The fluorescence intensity of L-Trp at 15 and 60 nm decreased, but there was no change in the spectrum when the quantity of hesperidin increased. This showed that hesperidin caused secondary structural alterations in the L-Trp residue at the interface, switching it from a hydrophilic to a hydrophobic environment.

Binding parameter: When equilibrium between the free and bound molecules has been attained following independent small molecule binding to a set of equivalent sites on macromolecules, the fluorescence intensities satisfy the following equation [39].

$$\log \frac{F_0 - F}{F} = \log K_a + n \log[Q] \quad (2)$$

where K_a is the binding constant; n is the number of binding sites per L-tryptophan molecules; and [Q] is the quencher concentration.

The binding constant (K_a) and the number of binding sites n can be determined by plotting log $(F_0 - F)/F$ *vs*. log K_a + n log [Q]. Compared to the amino acid-ligand complexes, which have binding constants ranging from 10^7 to 10^8 L mol^{-1}, hesperidin and L-Trp have moderate binding constants with affinities on the order 10^6 L mol^{-1}. With an increase in hesperidin concentration, K_a value decreases. This shows that the stability of these compounds reduces as their concentration increases.

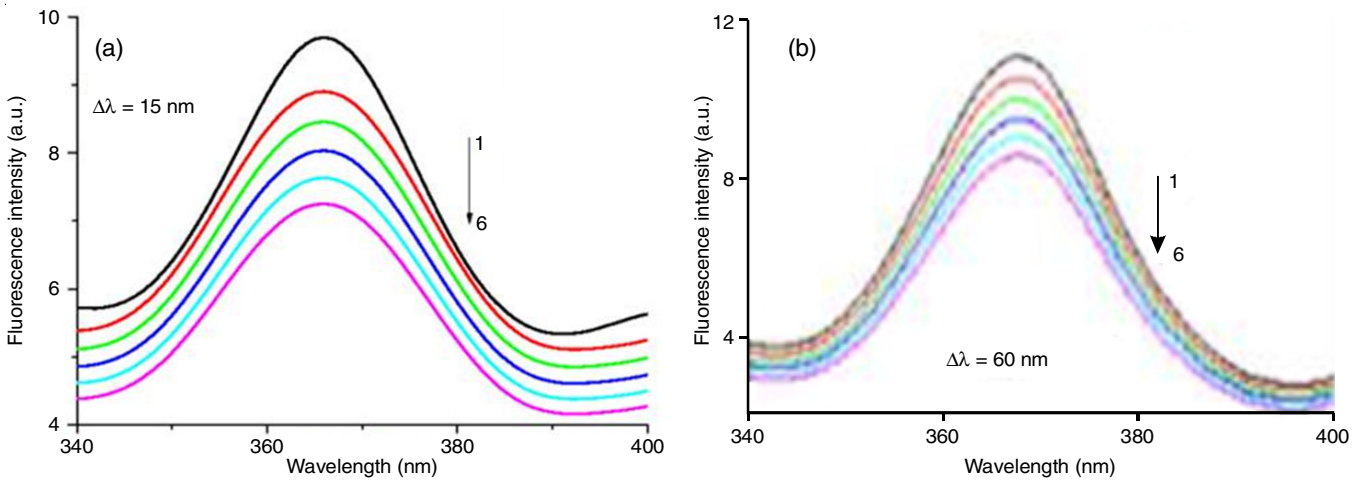

Fig. 3. Synchronous fluorescence spectra for L-tryptophan with hesperidin having (a) Δλ = 15 nm and (b) Δλ = 60 nm

It may be inferred by comparing the binding constants of various hesperidin conformations to L-Trp that the amount of positional hydroxyl and glycosylation are the primary structural characteristics that affect their ability to bind to L-Trp. The log plot of L-Trp with hesperidin showed an linear relationship with the following values: $K_a = 4.95 \times 10^6$ (L mol^{-1}), n = 1.53 and R = 0.99. The binding site was approximately 1, suggesting that hesperidin has a single binding site with an L-Trp interaction mechanism.

Time-resolved fluorescence spectra: The lifetime measurements were used to further corroborate the quenching processes for the interaction of hesperidin with L-Trp. Fig. 4 displays the time-resolved decay curves of L-Trp in both the presence and absence of flavonoids. The relative fluorescence lifespan of L-Trp is 3.18, 5.72 and 4.23 ns (2 = 1.27) while that of hesperidin at its maximum concentration is 1.22, 3.31 and 3.81 ns. The decay curves matched well to a bi-exponential function. The data fit a single exponential decay sum with a 2 value close to 1.27 nicely. Table-2 provides an overview of the decay parameters for all the systems. As seen in Fig. 4, there is no visible difference between the L-Trp decay curves with the increasing quantities of hesperidin. The following equation was used to determine the average lifetime (τ) for biexponential interactive fits based on decay times and relative amplitude (α).

$$\langle\tau\rangle = \frac{\tau_1\alpha_1^2 + \tau_2\alpha_2^2 + \tau_3\alpha_3^2}{\tau_1\alpha_1 + \tau_2\alpha_2 + \tau_3\alpha_3} \quad (3)$$

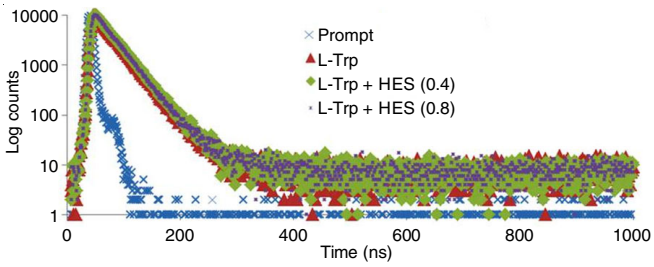

Fig. 4. Time-resolved fluorescence spectra of L-Trp with different concentrations of hesperidin (mol dm^{-5}) (1) 0.0, (2) 0.4 and (3) 0.8

The average fluorescence lifespan dropped from 3.20 ns to 3.05 ns with and without hesperidin, demonstrating that the mechanism is primarily static. The fluorescence lifetime values of L-Trp with and without various doses of hesperidin are shown in Table-2. The fluorescence lifetime of fluorophore is unaffected by the complex formation in case of static quenching. Therefore, it is safe to assume that all of the quenching processes of L-tryptophan with hesperidin fall under the category of static quenching with the complex formation.

Fluorescence resonance energy transfer (FRET): FRET is a way of transmitting energy between two chromophores based on their proximity to one another. The excitation energy is transferred from the donor to the acceptor during the ligand-protein interaction, preventing the donor molecule from emitting any photons. The following prerequisites must be met for this energy transfer. The molecule can emit fluorescence when acted as an energy donor; the donor's emission spectrum and the acceptor's absorbance spectrum overlap and their separation is smaller than 8 nm [40]. The overlap of the UV absorption spectrum of hesperidin with the fluorescence emission spectrum of L-Trp is shown in Fig. 5.

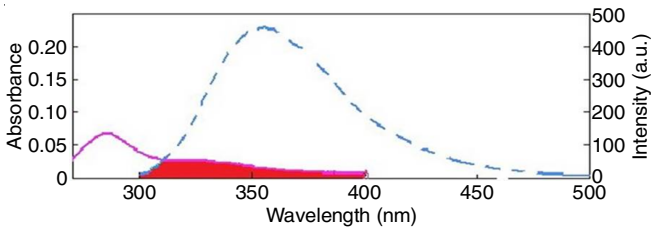

Fig. 5. Overlap of UV absorption spectra of hesperidin (solid line) with the fluorescence emission spectra of L-Trp (dotted line)

According to the spectral studies, L-Trp and hesperidin interacted. FRET could be used to measure the separation (r) between the bound hesperidin and L-Trp. Equation 4 was used to determine the energy transfer efficiency (E).

$$E = 1 - \frac{F}{F_O} = \frac{R_0^6}{R_0^6 + r_0^6} \quad (4)$$

where R_0 is the critical distance when the transfer efficiency is 50%; and r stands for the average separation between the donor and acceptor. The F and F_O are the fluorescence intensities of L-Trp in the presence and absence of hesperidin, respectively. The value J (2.49 10^{-15} cm^{-3} M^{-1}), which was computed using the overlapped component of the L-Trp emission spectrum and hesperidin absorption spectrum, is the overlap integral of the fluorescence emission spectrum of the donor and absorption spectrum of the acceptor. Since L-Trp and hesperidin were 8 nm apart, there is a strong possibility that energy can be transferred from L-Trp to hesperidin.

FTIR studies: L-Trp showed many distinctive peaks that might be connected to the existence of particular functional groups. Amide I, II and III were assessed in this investigation. The mid-infrared region, between 4000 and 400 cm^{-1}, of the infrared spectra was captured on a Fourier transform spectrometer. The IR absorption of the functional groups may vary over a broad range of the FTIR bands at 4000-1450 cm^{-1} due to the complicated interactions of atoms inside the molecule. The stretching vibrations between hydrogen and some extra atoms with a mass of 19 (or less) were responsible for the formation of strong abruption bands in the region of 4000 to 2,500 cm^{-1}

TABLE-2
FLUORESCENCE LIFETIME AND RELATIVE AMPLITUDES OF L-TRP WITH DIFFERENT CONCENTRATIONS OF HESPERIDIN

Concentration (M)	Lifetime (ns)			Average lifetime $\times 10^{-9}$ s	Relative amplitude			x^2	S.D. $\times 10^{-11}$ s		
	τ_1	τ_2	τ_3		B_1	B_2	B_3		T_1	T_2	T_3
L-Trp	3.18	5.72	4.23	3.20	88.28	6.49	5.23	1.27	9.11	3.95	5.59
L-Trp + HES (0.4)	2.96	3.84	5.03	3.18	51.53	42.40	6.08	1.38	1.31	1.17	5.12
L-Trp + HES (0.8)	1.22	3.31	3.81	3.05	3.10	91.22	5.67	1.27	1.60	1.65	7.63

in the functional group region. The spectrum of L-Trp features a broad and intensive band around 3361 cm^{-1} peak shift to 3367 cm^{-1} maybe due to the interaction of hesperidin with the OH band of L-Trp. The peak of L-trp 2927 cm^{-1} shifted to 2926 cm^{-1} C-H stretching whereas 2256 cm^{-1} peak shifted to 2132 cm^{-1} C=C stretching. The spectra of L-trp 1653 cm^{-1} peak shifted to 1651 cm^{-1} C=N stretching (Fig. 6).

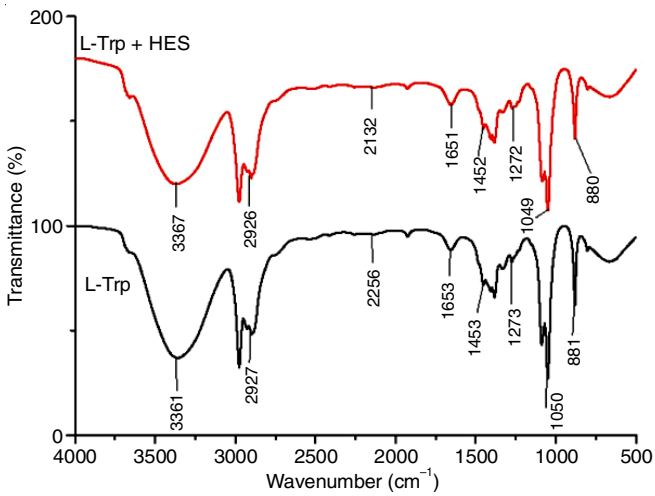

Fig. 6. FTIR spectra of L-tryptophan with hesperidin

Antibacterial activity: For the antibacterial assay, Gram-positive *S. aureus* and Gram-negative *E. coli* were chosen. The Muller Hinton broth was infected with the bacterial pathogens, which were then left to incubate for 24 h at 37 ºC. Using a cork borer, wells were created on 6 mm Muller Hinton agar plates and the bacterial cultures were spread out individually on the plates. Each well was filled with 100 µL of various samples dissolved in DMSO solvent, which were then incubated at 282 ºC for 24 h. To determine the zone of inhibition (ZOI) of pathogens, the agar well diffusion method was employed. L-Tryptophan and the compound of hesperidin significantly inhibited the growth of both Gram-positive and Gram-negative bacteria (Table-3).

TABLE-3
ANTIBACTERIAL ACTIVITY OF L-TRP WITH HESPERIDIN

Bacterial pathogen	Zone of inhibition (mm)		
	L-Trp	Hesperidin	L-Trp + HES
S. aureus	10	18	18
E. coli	18	18	19

Anticancer activity: Using the MTT technique, the anticancer activities of hesperidin extracts were assessed. HeLa, a human cervical cancer cell line, was cultured separately in 96-well plates at a density of 1×10^4 cells/well in MEM media with 1X antibiotic antimycotic solution and 10% fetal bovine serum (Himedia, India) in a CO_2 incubator at 37 ºC with 5% CO_2. The hesperidin extracts were then added. The cells were washed with 200 µL of 1X PBS, then the cells were treated with various test concentrations of the sample (HES) and with IC_{50} concentration of doxorubicin (12 µg/mL) as a positive control in serum-free media and incubated for 24 h.

Following the treatment, the medium was extracted from the cells. A solution of MTT at a concentration of 0.5 mg/mL, prepared in 1X PBS, was introduced into a CO_2 incubator and allowed to incubate at 37 ºC for 4 h. After the incubation period, the liquid containing MTT in the cells was taken out and the cells were washed with 200 mL of PBS. The synthesized crystals were thoroughly dissolved in a solution of 100 mL of DMSO. The assessment of color intensity was conducted at a wave-

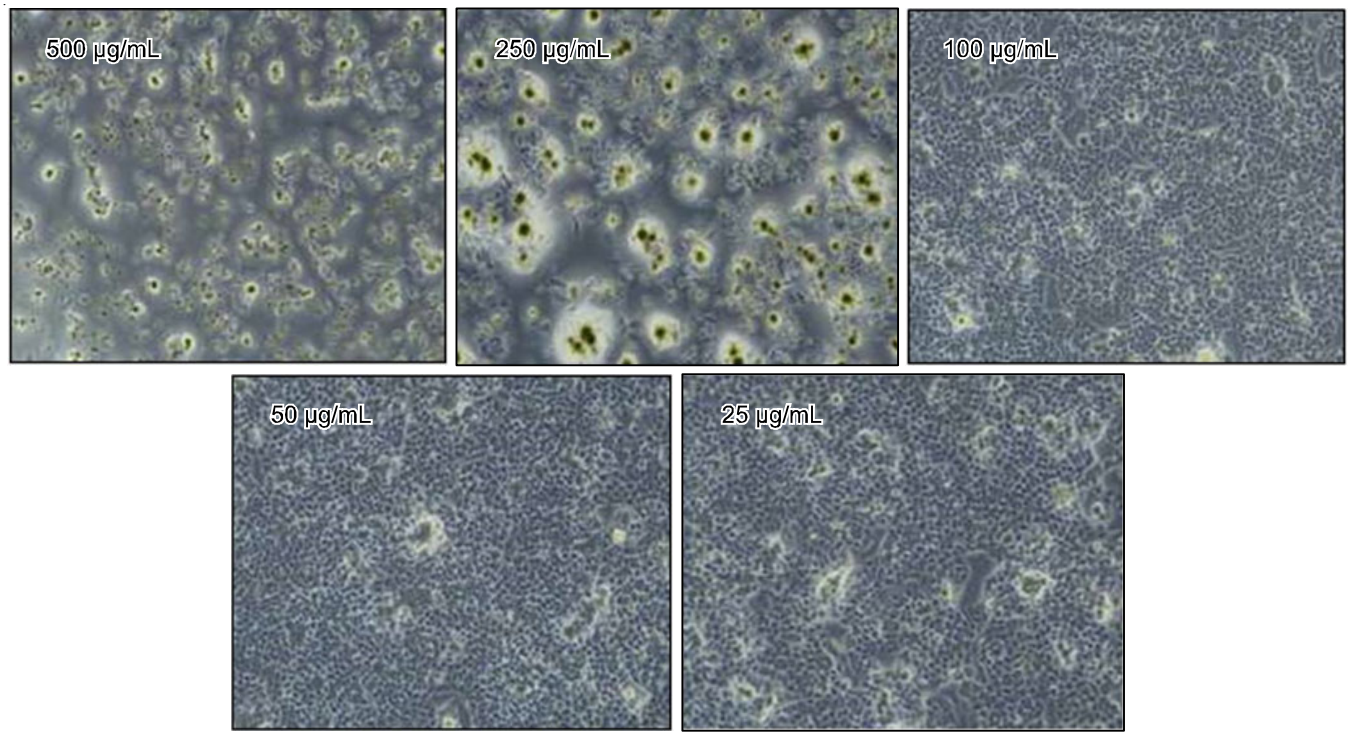

Fig. 7. Effect of hesperidin different concentrations on cell viability microscopic image of HeLa cell

length of 570 nm. The results of the anticancer activity on hesperidin in HeLa cervical cancer cells are presented in Fig. 7a-b.

Anticancer activity in the various concentrations using (25, 50, 100, 250 and 500 µg/mL) concentration *versus* cell viability is shown in Fig. 8. The graph shows that there is a positive relationship between the log concentration of the ethanol and extract and the percentage of inhibition of HeLa cervical cancer cells. it means that the higher concentration, the higher the percentage of inhibition on HeLa cells. Therefore the largest concentration of inhibition using 500 µg/mL. The antilog value of the IC_{50} value, which is the concentration needed to inhibit 50% growth of HeLa cervical cancer cells. Based on the calculation of the linear regression equation IC_{50} value was 193.5 ± 0.02 µg/mL (Fig. 9).

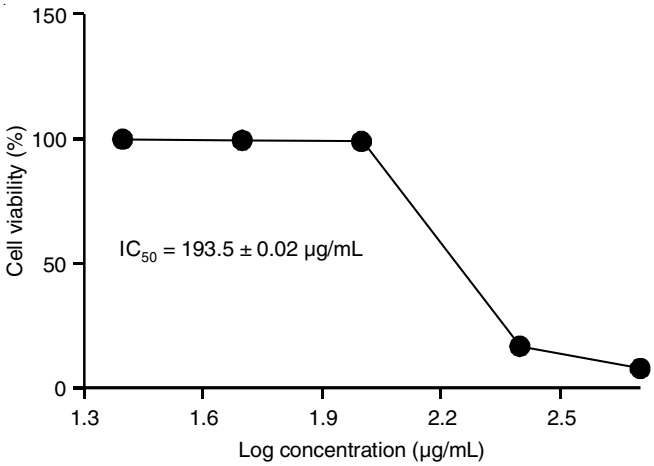

Fig. 9. IC_{50} curve

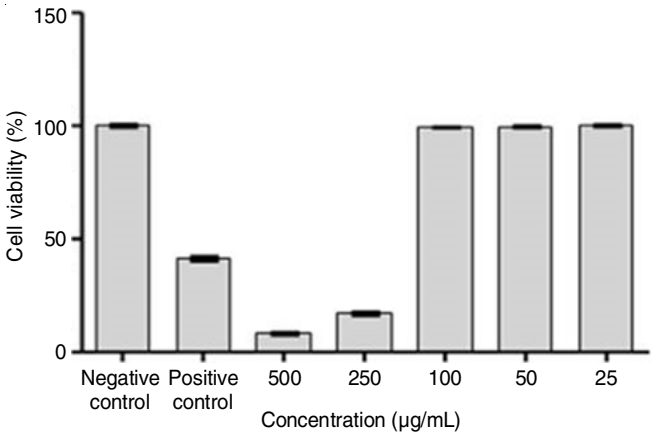

Fig. 8. L-Tryptophan with hesperidin induced apoptosis and cell cycle arrest in HeLa cells cells

Molecular docking: The protein data bank (PDB) was used to derive the first three-dimensional [3D] structures for *S. aureus* ATCC 25923 (PDB ID: 1JIJ), *E. coli* ATCC 25922 (PDB ID: 2I68) and hesperidin (PubChem ID: 10621). Auto dock vina software and auto dock tools were used while docking. The molecular docking results are shown in Figs. 10 and 11.

Root mean square deviation (RMSD) values varied between 1 and 2 and the binding pattern was retained. The grid map points for *S. aureus* and *E. coli* with HES were 24, 24 and 24, respectively. By searching for the best active regions for the protein-ligand interactions, we hope to identify the hydrogen binding interactions that take place between ligand-receptor complexes [41]. The population size in this case was about 150 and the maximum number of generations was roughly 27000. The Lamarckian genetic algorithm (LGA) was applied. The docking results against *S. aureus* with hesperidin and *E. coli* with hesperidin, protein indicated a well-conserved binding region but with a slightly predicted best binding energy value. The calculated binding energy and the inhibition constant values are presented in Table-4.

The best free binding energy was found for *S. aureus* with hesperidin (-10.5 kcal/mol) and *E. coli* with hesperidin (-9.5 kcal/mol). The above information indicated that the stabilization at the binding cavity of *S. aureus* with hesperidin and *E. coli* with hesperidin complex was mostly due to the residues. HIS A:47, GLY A:49, HIS A:50, LEU A:70, THR A: 75, LYS A:84, TYR A:96, GLY A:98, ALA A:99, ASP A:177, ASP A:195, GLN A:196, PRO A:222, PHE A:232 and ASN A:20, GLY A:23, TYR A:67, GLN A:150, MET A: 196, SER A:197,

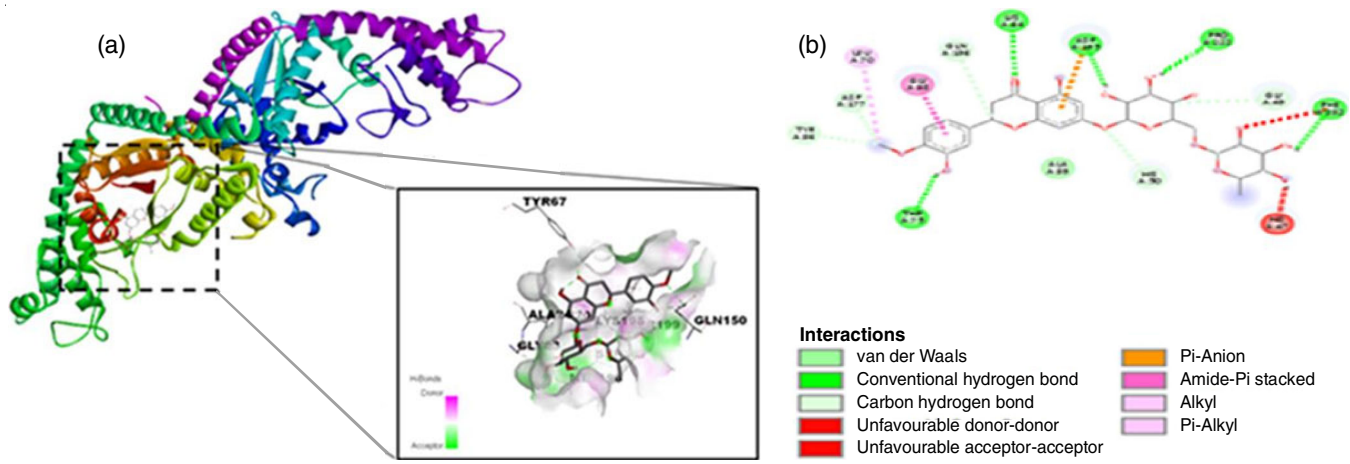

Fig. 10. (a) Docked complex of tyrosyl-tRNA synthetase from *Staphylococcus aureus* with hesperidin, (b) 2D interaction plot of docked complex of tyrosyl-tRNA synthetase from *Staphylococcus aureus* with hesperidin

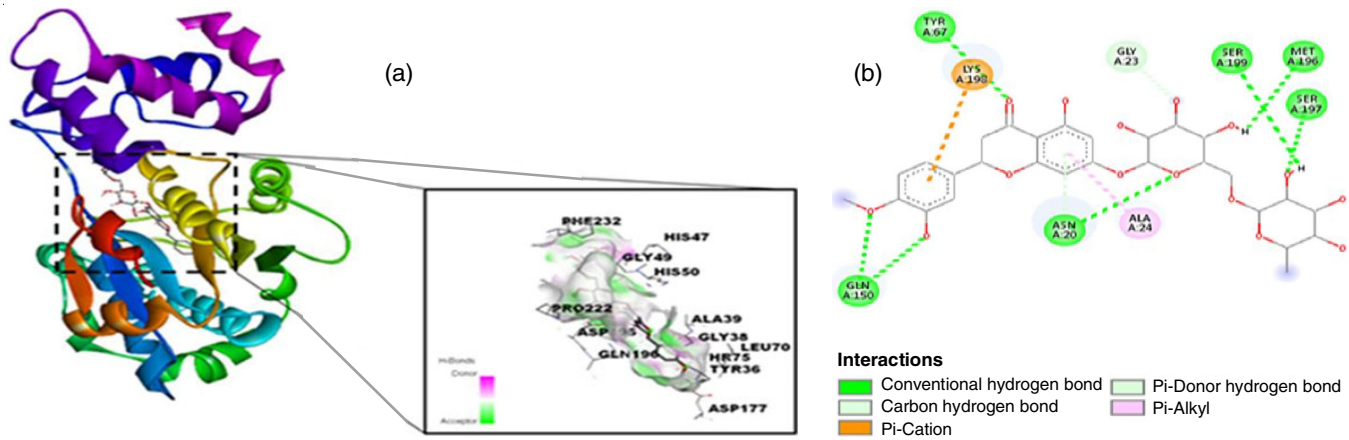

Fig. 11. (a) Docked complex of tryptophanyl-tRNA synthetase from *Escherichia coli* with hesperidin, (b) 2D interaction plot of docked complex of tryptophanyl-tRNA synthetase from *Escherichia coli* with hesperidin

TABLE-4
BINDING ENERGY (ΔE, kcal/mol) AND RMSD (Å) OF *S. aureus*, *E. coli* WITH HESPERIDIN

PDB code	Biological source	Protein name	RMSD (Å)	Binding energy (ΔE, kcal/mol)
1JIJ	*Staphylococcus aureus*	Tyrosyl-tRNA synthetase (TyrRS)	3.2	-10.5
5VOI	*Escherichia coli*	Tryptophanyl-tRNA synthetase	1.90	- 9.5

LYS A:198, SER A:199. The hydrogen bond between the active site residue of *S. aureus* with CGA and *E. coli* with CGA was also observed for interaction analysis.

Conclusion

Under the simulated physiological conditions, the interaction of L-Trp and hesperidin has been studied *in vitro* by various spectral techniques. The static quenching occured due to the formation of complex formation where hesperidin quenches L-Trp. Results from fluorescence spectroscopy and UV-vis absorption showed that the binding constants of flavonoids to L-Trp are moderate. The hydrogen bonding, electrostatic contacts and hydrophobic interactions are the main types of intermolecular interactions that flavonoids use to attach to L-Trp. In the hesperidin and L-Trp systems, the synchronous fluorescence spectroscopy reveals an increase in polarity and a decrease in hydrophobic properties near Trp residues, but in the Tyr residue microenvironment, there is no change.

CONFLICT OF INTEREST

The authors declare that there is no conflict of interests regarding the publication of this article.

REFERENCES

1. A.L. Desai, K. Bhatt, K.M. Modi, N.P. Patel, M. Panchal, A. Kongor, C.N. Patel and A. Liška, *Chem. Phys.*, **554**, 111426 (2022); https://doi.org/10.1016/j.chemphys.2021.111426
2. R.M. Callejón, A.M. Troncoso and M.L. Morales, *Talanta*, **81**, 1143 (2010); https://doi.org/10.1016/j.talanta.2010.02.040
3. Q.S. Qu, X.Q. Tang, C.Y. Wang, G.J. Yang, X.Y. Hu, X. Lu, Y. Liu, S.C. Li and C. Yan, *Anal. Chim. Acta*, **572**, 212 (2006); https://doi.org/10.1016/j.aca.2006.05.026
4. X.S. Zhu, A.Q. Gong, B.S. Wang and S.H. Yu, *J. Lumin.*, **128**, 1815 (2008); https://doi.org/10.1016/j.jlumin.2008.05.002
5. F. Wang and W. Huang, *J. Pharm. Biomed. Anal.*, **43**, 393 (2007); https://doi.org/10.1016/j.jpba.2006.07.007
6. P. Bandyopadhyay and K. Saha, *Chem. Phys. Lett.*, **457**, 227 (2008); https://doi.org/10.1016/j.cplett.2008.03.076
7. N. Shao, J.Y. Jin, S.M. Cheung, R.H. Yang, W.H. Chan and T. Mo, *Angew. Chem. Int. Ed.*, **45**, 4944 (2006); https://doi.org/10.1002/anie.200600112
8. X. Yang, Y. Guo and R.M. Strongin, *Angew. Chem. Int. Ed.*, **50**, 10690 (2011); https://doi.org/10.1002/anie.201103759
9. W. Hao, A. McBride, S. McBride, J.P. Gao and Z.Y. Wang, *J. Mater. Chem.*, **21**, 1040 (2011); https://doi.org/10.1039/C0JM02497J
10. K. Liu, L. He, X. He, Y. Guo, S. Shao and S. Jiang, *Tetrahedron Lett.*, **48**, 4275 (2007); https://doi.org/10.1016/j.tetlet.2007.04.042
11. L.D. Li, Z.B. Chen, H.T. Zhao and L. Guo, *Biosens. Bioelectron.*, **26**, 2781 (2011); https://doi.org/10.1016/j.bios.2010.10.041
12. Y. Shimazaki, T. Yajima, M. Takani and O. Yamauchi, *Coord. Chem. Rev.*, **253**, 479 (2009); https://doi.org/10.1016/j.ccr.2008.04.012
13. C.X. Tang, N.N. Bu, X.W. He and X.B. Yin, *Chem. Commun.*, **47**, 12304 (2011); https://doi.org/10.1039/c1cc15323d
14. R.H. McMenamy and J.L. Oncley, *J. Biol. Chem.*, **233**, 1436 (1958); https://doi.org/10.1016/S0021-9258(18)49353-2
15. R.H. McMenamy, *Arch. Biochem. Biophys.*, **103**, 409 (1963); https://doi.org/10.1016/0003-9861(63)90430-2
16. R.H. McMenamy, *J. Biol. Chem.*, **239**, 2835 (1964); https://doi.org/10.1016/S0021-9258(18)93822-6
17. R.H. McMenamy, *J. Biol. Chem.*, **240**, 4235 (1965); https://doi.org/10.1016/S0021-9258(18)97049-3
18. T.P. King and M. Spencer, *J. Biol. Chem.*, **245**, 6134 (1970); https://doi.org/10.1016/S0021-9258(18)62672-9
19. G.F. Fairclough Jr. and J.S. Fruton, *Biochemistry*, **5**, 673 (1966); https://doi.org/10.1021/bi00866a038
20. J.R. Lakowicz, Principles of Fluorescence Spectroscopy, Springer, Boston, MA, USA, edn. 3 (2006).
21. R. Sridharan, J. Zuber, S.M. Connelly, E. Mathew and M.E. Dumont, *Biochim. Biophys. Acta Biomembr.*, **1838**, 15 (2014); https://doi.org/10.1016/j.bbamem.2013.09.005

22. B.Y. Silber and J.A.J. Schmitt, *Neurosci. Biobehav. Rev.*, **34**, 387 (2010); https://doi.org/10.1016/j.neubiorev.2009.08.005
23. S. Löb, A. Königsrainer, H.G. Rammensee, G. Opelz and P. Terness, *Nat. Rev. Cancer*, **9**, 445 (2009); https://doi.org/10.1038/nrc2639
24. M. Kia, A. Islamnezhad, S. Shariati and P. Biparva, *Korean J. Chem. Eng.*, **28**, 2064 (2011); https://doi.org/10.1007/s11814-011-0066-9
25. J.W. Longworth, Excited States of Proteins and Nucleic Acids, in eds.: R.F. Steiner and I. Weinry, Excited States of Proteins and Nucleic Acids, Plenum Press: New York, Chap. 6, pp. 319-484 (1971).
26. A.M. Myint, Y.K. Kim, R. Verkerk, S. Scharpé, H. Steinbusch and B. Leonard, *J. Affect. Disord.*, **98**, 143 (2007); https://doi.org/10.1016/j.jad.2006.07.013
27. Y. Yang, J. Wolfram, H. Shen, X. Fang, and M. Ferrari, *Eur. J. Med. Chem.*, **58**, 390 (2012); https://doi.org/10.1016/j.ejmech.2012.10.028
28. M.S. Antunes, C.R. Jesse, J.R. Ruff, D. de Oliveira Espinosa, N.S. Gomes, E.E.T. Altvater, F. Donato, R. Giacomeli and S.P. Boeira, E.ET, *Eur. J. Pharmacol.*, **789**, 411 (2016); https://doi.org/10.1016/j.ejphar.2016.07.042
29. V. Gaur and A. Kumar, *Pharmacol. Rep.*, **62**, 635 (2010); https://doi.org/10.1016/S1734-1140(10)70321-2
30. A. Umeno, M. Horie, K. Murotomi, Y. Nakajima and Y. Yoshida, *Molecules*, **21**, 708 (2016); https://doi.org/10.3390/molecules21060708
31. M.S. Antunes, A.T.R. Goes, S.P. Boeira, M. Prigol and C.R. Jesse, *Nutrition*, **30**, 1415 (2014); https://doi.org/10.1016/j.nut.2014.03.024
32. W.C. Willett, *Science*, **296**, 695 (2002); https://doi.org/10.1126/science.1071055
33. G. Mazza, *Ann. Ist. Super. Sanita*, **43**, 369 (2007).
34. A.M. Mahmoud, M.B. Ashour, A. Abdel-Moneim and O.M. Ahmed, *J. Diabetes Complications*, **26**, 483 (2012); https://doi.org/10.1016/j.jdiacomp.2012.06.001
35. S.R.K.M. Hewage, M.J. Piao, K.A. Kang, Y.S. Ryu, X. Han, M.C. Oh, U. Jung, I.G. Kim and J.W. Hyun, *Biomol. Ther.*, **24**, 312 (2016); https://doi.org/10.4062/biomolther.2015.139
36. N. Polat, O. Ciftci, A. Cetin and T. Yilmaz, *Cutan. Ocul. Toxicol.*, **35**, 1 (2016); https://doi.org/10.3109/15569527.2014.999080
37. X. Yu, Z. Liao, B. Jiang, X. Hu and X. Li, *Spectrochim. Acta A Mol. Biomol. Spectrosc.*, **137**, 129 (2015); https://doi.org/10.1016/j.saa.2014.08.098
38. Y.K. Manea, A. Banu, M.T. Qashqoosh, M. Khan, F.M. Alahdal, A.A. Wani and S. Naqvi, *Chem. Phys.*, **546**, 111139 (2001); https://doi.org/10.1016/j.chemphys.2021.111139
39. X. Fan, S. Liu and Y. He, *Colloids Surf. B Biointerfaces*, **88**, 23 (2011); https://doi.org/10.1016/j.colsurfb.2011.05.029
40. B.L. Wang, D.Q. Pan, S.B. Kou, Z.Y. Lin and J.-H. Shi, *Chem. Phys.*, **530**, 110641 (2020); https://doi.org/10.1016/j.chemphys.2019.110641
41. N. Mani, S. Suresh, M. Govindammal, S. Kannan, E.I. Paulraj, D. Nicksonsebastin and M. Prasath, *Chem. Phys. Impact*, **7**, 100254 (2023); https://doi.org/10.1016/j.chphi.2023.100254